Optik - International Journal for Light and Electron Optics 271 (2022) 170127

Contents lists available at ScienceDirect

Optik - International Journal for Light and Electron Optics

journal homepage: www.elsevier.com/locate/ijleo

Original research article

Optical solitons for Radhakrishnan–Kundu–Lakshmanan equation in the presence of perturbation term and having Kerr law

Neslihan Ozdemir

Department of Software Engineering, Istanbul Gelisim University, Istanbul, Turkey

ARTICLE INFO

Keywords:
The generalized projective Riccati equations
A simple version of new extended auxiliary equation
Unified Riccati equation expansion
Soliton
Parameter effect

ABSTRACT

Purpose: In this research study, obtaining the analytical and soliton solutions to the perturbed Radhakrishnan–Kundu–Lakshmanan (RKL) equation with Kerr law nonlinearity is aimed via the generalized projective Riccati equations method (GPREM), a simple version of the new extended auxiliary equation method (SAEM26), and unified Riccati equation expansion method (UREEM). At the same time, the roles of some parameters included in the perturbed RKL equation on soliton dynamics are analyzed.
Methodology: The presented methods are successfully employed to the perturbed RKL equation. In the application of the presented methods, to convert the perturbed RKL equation into a nonlinear ordinary differential equation, we choose suitable complex wave transformation for the proposed model. Later, a linear equation system is derived using the GPREM, SAEM26, and UREEM, the system is solved, the appropriate solution sets are obtained, and the soliton solutions are achieved, respectively.
Findings: The singular, bright and dark soliton solutions are generated by choosing the suitable set and parameter values. To comprehend the physical dynamics of some solutions, 3D, contour, and 2D graphs are demonstrated. In addition, 2D graphs are drawn to show how some parameters in the main equation have an effect on soliton behaviors. The examination indicates that the model parameters have a substantial effect on the soliton dynamics. Depending on the soliton forms, the effect can be varied. The results presented in this paper will be useful for future works in soliton theory and the presented methods can be effectively implemented to such equations.
Originality: The effects of the model parameters included in the perturbed RKL equation on soliton dynamics are analyzed for the first time in this study.

1. Introduction

Modeling of nonlinear evolution equations (NLEEs) emerges in many scientific areas like quantum mechanics, biology, plasma physics, nonlinear optics, fluid dynamics and hydrodynamics. Various NLEEs form the basis for modeling the dynamics of soliton propagation through an optical waveguide. Soliton theory has a wide range of implementations in nonlinear physics fields [1–6]. Obtaining the analytical solutions of NLEEs is an important field of study in recent years to better understand complex phenomena. With the development of soliton theory, several approaches have been improved by researchers to solve NLEEs, such as the modified simple equation technique [7–9], sine-Gordon expansion scheme [10–15], the modified Kudryashov method [16,17], the improved F-expansion method [18,19], the exp-function expansion scheme [20], the modified extended tanh expansion method [21], new Kudryashov and the unified Riccati equation expansion [22], the Riccati Bernoulli sub-ODE approach [23,24], the first integral

E-mail address: neozdemir@gelisim.edu.tr.

https://doi.org/10.1016/j.ijleo.2022.170127
Received 16 September 2022; Received in revised form 18 October 2022; Accepted 18 October 2022
Available online 25 October 2022
0030-4026/

scheme [25–27], enhanced modified tanh expansion technique [28], the Hirota bilinear method [29], the F-expansion scheme [30], Laplace–Adomian decomposition approach [31].

Since optical solitons have the characteristics of being carriers over long distances without changing their shape and without any attenuation in their amplitudes, they are of great importance in today's telecommunication field and many models of optical solitons have been developed. Such as, Biswas–Milovic [22], Chen–Lee–Liu [32], Kundu–Mukherjee–Naskar [33,34], Kundu–Eckhaus [35], Schrödinger–Hirota [36], Lakshmanan–Porsezian–Daniel [37–40], Biswas–Arshed [41], Manakov [42] and Sasa–Satsuma equation [43,44]. Kerr is important because depending on the Kerr two solitons affect each other annihilate, merge or create many new solitons. But study on the equations that having Kerr, is not simple without taking into account some special methods like perturbation technique or variational method. The RKL model that describes the soliton dynamics via a polarization-preserving fiber is one of the samples of the mathematical models. This model is the known nonlinear Schrödinger equation which is handled with a couple of perturbations because of the self-steepening and third-order distribution (3OD) effect. This equation firstly emerged in 1999 [45].

The generalized Radhakrishnan–Kundu–Lakshmanan equation is defined as follows [46]:

$$i\Psi_t + \alpha\Psi_{xx} + \beta F\left(|\Psi|^2\right)\Psi = i\lambda\left\{F\left(|\Psi|^2\right)\Psi\right\}_x - i\delta\Psi_{xxx}. \tag{1}$$

The general form of perturbed Radhakrishnan–Kundu–Lakshmanan equation having nonlinearity is given as [47]:

$$i\Psi_t + \alpha\Psi_{xx} + \beta F\left(|\Psi|^2\right)\Psi = i\tau\Psi_x + i\lambda\left\{F\left(|\Psi|^2\right)\Psi\right\}_x + i\gamma\left\{F\left(|\Psi|^2\right)\right\}_x\Psi - i\delta\Psi_{xxx}, \tag{2}$$

in which $\Psi(x,t)$ denotes the function of the complex-valued wave with spatial variable x and temporal variable t. Besides, F is the real-valued algebraic function that determines the type of nonlinearity. The coefficients α and β represent the group-velocity dispersion (GVD) and the nonlinearity terms, respectively. Moreover, τ indicates the coefficient of inter-modal dispersion, and λ specifies the coefficient of the self-steepening for short pulses. Furthermore, γ and δ describe the coefficients of the higher-order dispersion term and the third-order dispersion (TOD) term, respectively. Herein, the interaction between GVD and TOD is very important. When the GVD closes to zero, in order to keep and improve the performance of the pulse interaction along trans-oceanic distances, it should be needed to consider the third-order dispersions. As the GVD changes, it should be considered the higher order dispersion terms [48]. The perturbed RKL equation is one of the substantial models to represent short pulse propagation in optical fiber [48]. That is, the model is utilized so that solitons' propagation is modeled via optical fiber.

In the literature, various methods have been applied to the generalized Radhakrishnan–Kundu–Lakshmanan equation deriving different types of soliton solutions, such as the $(-\psi(q))$ method [46], the ansatz of solitary wave [48], the modified simple equation and the extended simplest equation techniques in [49], the improved modified extended tanh-function approach in [50]. The perturbed RKL equation has been examined by some researchers in recent years. To acquire the analytical solutions for Eq. (2), the generalized exponential rational function approach was implemented in [51]. Various kinds of soliton solutions to the perturbed RKL equation were derived through the modified extended tanh expansion approach enhanced with the new Riccati solutions in [52]. For the perturbed RKL equation with considering Kerr law and power law nonlinearity, dark, bright, singular soliton solutions were retrieved utilizing trial equation approach and modified simple equation technique in [53], the extended trial function approach in [54]; besides, chirp-free bright soliton solutions were revealed with the aid of traveling wave hypothesis in [55].

The UREEM is one of the powerful technique in order to solve the NLEEs. Using this approach, Sirendaoreji acquired the exact traveling wave solutions of two novel classes of Benjamin–Bona–Mahony models [56] and Zayed et al. retrieved dark, bright, singular solitons in magneto-optic waveguides [57]. Another robust method is the GPREM that has been studied by some researchers. For example, with the help of this approach, several types of soliton solutions were produced for Lakshmanan–Porsezian–Daniel model in [58] and for the generalized Zakharov–Kuznetsov equation in [59]. SAEM26 is another effective approach that is utilized to obtain analytical solutions proposed in [60].

The purpose of this paper is to enforce three efficient methods, namely GPREM, SAEM26, UREEM in constructing the analytical solutions and analyze the effect of parameters on the obtained solutions for the perturbed RKL equation having Kerr law nonlinearity by considering the $F(G) = G$ as follows:

$$i\Psi_t + \alpha\Psi_{xx} + \beta|\Psi|^2\Psi = i\tau\Psi_x + i\lambda\left(|\Psi|^2\Psi\right)_x + i\gamma\left(|\Psi|^2\right)_x\Psi - i\delta\Psi_{xxx}. \tag{3}$$

By now, the presented methods have not been employed to the perturbed Radhakrishnan–Kundu–Lakshmanan equation in the literature. In this paper, it is aimed to indicate that these methods are alternative approaches for examining nonlinear partial differential equations. It is aimed to successfully demonstrate that the proposed methods are not only easy to use and effective methods for nonlinear partial differential equations, but also for higher order and dispersive optic problems. Furthermore, it is aimed to investigate how have the effects of the model parameters on soliton dynamics.

The organization of the rest of this article is as follows: In Section 2, nonlinear ordinary differential form of the Eq. (3) is presented. GPREM is described, and its implementation to Eq. (3) is offered in Section 3. We submit a summary the SAEM26 and its enforcement for Eq. (3) in Section 4. We represent a brief and application to the perturbed RKL model of UREEM in Section 5. Some results are discussed and, graphical visualizations are demonstrated in Section 6. In the last section, we present the conclusion.

2. Nonlinear ordinary differential form of the perturbed RKL equation

Firstly, take into account the following wave transformations:

$$\Psi(x,t)=\Theta(\eta)e^{i\psi},\eta=x-\omega t,\psi=-\kappa x-vt+\theta, \tag{4}$$

where κ, v, θ, and ω are non-zero constants. Herein, $\Theta(\eta)$ is the shape of the soliton pulse, η is a new variable, ω is the velocity, ψ represents the phase-component, θ is defined as the phase-constant, κ denotes the frequency, and v is the parameter of wave number. Inserting Eq. (4) into Eq. (3), we derived the following nonlinear ordinary differential equations (NODEs) from the real and imaginary parts, respectively:

$$-(3\tau+3\omega+6\alpha\kappa+9\kappa^2\delta)\Theta(\eta)-(3\lambda+2\gamma)\Theta^3(\eta)+3\delta\frac{d^2\Theta(\eta)}{d\eta^2}=0 \tag{5}$$

and

$$(v+\alpha\kappa^2+\delta\kappa^3+\tau\kappa)\Theta(\eta)+(\beta-\lambda\kappa)\Theta^3(\eta)+(\alpha+3\delta\kappa)\frac{d^2\Theta(\eta)}{d\eta^2}=0. \tag{6}$$

Considering that $\Theta(\eta)$ satisfies both Eq. (5), and Eq. (6), the following constraint conditions are acquired:

$$\beta=\frac{-6\kappa\lambda\delta-6\delta\gamma\kappa-3\alpha\lambda+2\gamma\alpha}{3\delta}, \tag{7}$$

$$\omega=\frac{-8\delta^2\kappa^3-8\kappa^2\delta\alpha-2\alpha^2\kappa-2\kappa\tau\delta-\alpha\tau+\delta v}{3\delta\kappa+\alpha}. \tag{8}$$

In this study, we consider Eq. (6) as a NODE form of Eq. (3).

3. Sketch and practice of the GPREM to the perturbed RKL equation

In this section, the GPREM [61,62] is summarized and the application to Eq. (3) is given.

3.1. Sketch of the GPREM to the perturbed RKL equation

Step 1: Assume that Eq. (6) has a solution of the following form:

$$\Psi(\eta)=A_0+\sum_{k=1}^{N}\Theta(\eta)^{k-1}\left[A_k\Theta(\eta)+B_k\Omega(\eta)\right], \tag{9}$$

in which A_0, A_k and B_k are constants to be calculated. Herein, N is the balancing constant. $\Theta(\eta)$ and $\Omega(\eta)$ satisfy the following ODEs:

$$\Theta'(\eta)=\epsilon\Theta(\eta)\Omega(\eta), \tag{10}$$

$$\Omega'(\eta)=\sigma+\epsilon\Omega(\eta)^2-\mu\Theta(\eta),\epsilon=\pm1, \tag{11}$$

where

$$\Omega(\eta)^2=-\epsilon\left(\sigma-2\mu\Theta(\eta)+\frac{\mu^2+r}{\sigma}\Theta(\eta)^2\right). \tag{12}$$

Herein, μ and σ are nonzero constants. If $\mu=\sigma=0$, Eq. (9) has the following solution:

$$\Psi(\eta)=\sum_{k=1}^{N}A_k\Omega^k(\eta), \tag{13}$$

in which $\Omega(\eta)$ satisfies the given ODE:

$$\Omega'(\eta)=\Omega^2(\eta). \tag{14}$$

Step 3: The positive integer N in Eq. (9) is calculated utilizing from the classical balancing rule in Eq. (6).

Step 4: Inserting Eq. (9) along with Eqs. (10)–(12) into Eq. (6), gathering all terms of the identical order of $\Theta^k(\eta)\Omega^l(\eta)$ $(k,l=0,1,2,\ldots)$ and taking each to zero, we procure a set of algebraic equations whose solutions yield the parameters of $A_0, A_k, B_k, \mu, r, \sigma$.

Step 5: Eq. (10) and Eq. (11) have the following solutions:

Family 1: If $\epsilon=-1, r=-1$, and $\sigma>0$, we get,

$$\Theta_1(\eta)=\frac{\sigma sech\left(\sqrt{\sigma}\eta\right)}{\mu sech\left(\sqrt{\sigma}\eta\right)+1},\quad \Omega_1(\zeta)=\frac{\sqrt{\sigma}tanh\left(\sqrt{\sigma}\eta\right)}{\mu sech\left(\sqrt{\sigma}\eta\right)+1}. \tag{15}$$

Family 2: If $\epsilon = -1, r = 1$, and $\sigma > 0$, we get,

$$\Theta_2(\eta) = \frac{\sigma csch\left(\sqrt{\sigma}\eta\right)}{\mu csch\left(\sqrt{\sigma}\eta\right)+1}, \quad \Omega_2(\eta) = \frac{\sqrt{\sigma}coth\left(\sqrt{\sigma}\eta\right)}{\mu csch\left(\sqrt{\sigma}\eta\right)+1}. \tag{16}$$

Family 3: If $\epsilon = 1, r = -1$, and $\sigma > 0$, we get,

$$\Theta_3(\eta) = \frac{\sigma sec\left(\sqrt{\sigma}\eta\right)}{\mu sec\left(\sqrt{\sigma}\eta\right)+1}, \quad \Omega_3(\eta) = \frac{\sqrt{\sigma}tan\left(\sqrt{\sigma}\eta\right)}{\mu sec\left(\sqrt{\sigma}\eta\right)+1}. \tag{17}$$

$$\Theta_4(\eta) = \frac{\sigma csc\left(\sqrt{\sigma}\eta\right)}{\mu csc\left(\sqrt{\sigma}\eta\right)+1}, \quad \Omega_4(\eta) = \frac{\sqrt{\sigma}cot\left(\sqrt{\sigma}\eta\right)}{\mu csc\left(\sqrt{\sigma}\eta\right)+1}. \tag{18}$$

Family 4: If $\mu = \sigma = 0$, we get,

$$\Theta_5(\eta) = \frac{K}{\eta}, \quad \Omega_5(\eta) = \frac{1}{\epsilon\eta}. \tag{19}$$

where K is a nonzero constant.

Step 6: Utilizing the parameters of $A_0, A_k, B_k, \mu, r, \sigma$ and Eqs. (15)–(19) by considering Eq. (4), the solutions of Eq. (3) are acquired.

3.2. Practice of the GPREM to the perturbed RKL equation

Utilizing the relation between the nonlinear term and the term that involves the highest order derivative in Eq. (6), we acquire $N = 1$. So, the proposed solution in Eq. (9) degenerates into the following form:

$$\Psi(\eta) = A_0 + A_1\Theta(\eta) + B_1\Omega(\eta). \tag{20}$$

Inserting Eq. (20) and its necessary derivatives by considering Eq. (10) and Eq. (11) into Eq. (6) and assuming each coefficients of same power of $\Theta^i(\eta)\Omega^j(\eta)$ as zero, an algebraic equation system is derived. After solving this system, the following solution sets are obtained:

Family 1: Considering $\epsilon = -1$ and $r = -1$ in the algebraic system, the following result is derived:

Result 1:

$$\sigma = -\frac{2\Upsilon_1}{\xi\left(3\kappa\delta+\alpha\right)}, A_0 = 0, A_1 = -\frac{\sqrt{-3\Upsilon_1\delta\left(3\delta\kappa+1\right)\left(\mu^2-1\right)}}{2\Upsilon_1}, B_1 = \frac{\sqrt{6\xi\delta}}{2\xi}, \tag{21}$$

where $\xi = 2\gamma+3\lambda$, $\Upsilon_1 = \xi\left(\delta\kappa^3+\alpha\kappa^2+\kappa\tau+\nu\right)$. Inserting the parameters in Eq. (21) into Eq. (20) taking into account Eq. (15)-Eq. (19) and Eq. (4), we produce the solution of Eq. (3) as:

$$\Psi_{1,1} = \frac{\left(-B_1\sqrt{\sigma}\,\sinh\left(\frac{\sqrt{\sigma}\left(\omega_1 t - x(3\kappa\delta+\alpha)\right)}{3\kappa\delta+\alpha}\right)+\sigma A_1\right)\mathrm{e}^{\mathrm{i}(-\kappa x+\nu t+\theta)}}{\mu+\cosh\left(\frac{\sqrt{\sigma}\left(\omega_1 t - x(3\kappa\delta+\alpha)\right)}{3\kappa\delta+\alpha}\right)}, \tag{22}$$

where $\omega_1 = -8\delta^2\kappa^3 + \left(-8\alpha\kappa^2 - 2\kappa\tau + \nu\right)\delta - 2\alpha^2\kappa - \tau\alpha$.

Family 2: Considering $\epsilon = -1$ and $r = 1$ in the algebraic system, the following result is retrieved:

Result 2:

$$\sigma = -\frac{2\Upsilon_1}{\xi\left(3\kappa\delta+\alpha\right)}, A_0 = 0, A_1 = -\frac{\sqrt{-3\Upsilon_1\delta\left(3\delta\kappa+\alpha\right)\left(\mu^2+1\right)}}{2\Upsilon_1}, B_1 = \frac{\sqrt{6\xi\delta}}{2\xi}. \tag{23}$$

Inserting the parameters in Eq. (23) into Eq. (20) taking into account Eq. (15)-Eq. (19) and Eq. (4), we acquire the solution of Eq. (3) as:

$$\Psi_{1,2} = \frac{\mathrm{e}^{\mathrm{i}(-\kappa x+\nu t+\theta)}\left(B_1\sqrt{\sigma}\,\cosh\left(\frac{\left(\omega_1 t - x(3\kappa\delta+\alpha)\right)\sqrt{\sigma}}{3\kappa\delta+\alpha}\right)+\sigma A_1\right)}{\mu-\sinh\left(\frac{\left(\omega_1 t - x(3\kappa\delta+\alpha)\right)\sqrt{\sigma}}{3\kappa\delta+\alpha}\right)}. \tag{24}$$

Family 3: Considering $\epsilon = 1$ and $r = -1$ in the algebraic system, the following result is derived:

$$\sigma = -\frac{2\Upsilon_1}{\xi\left(3\kappa\delta+\alpha\right)}, A_0 = 0, A_1 = -\frac{\sqrt{-3\Upsilon_1\delta\left(3\delta\kappa+\alpha\right)\left(\mu^2-1\right)}}{2\Upsilon_1}, B_1 = \frac{\sqrt{6\xi\delta}}{2\xi}. \tag{25}$$

Inserting the parameters in Eq. (23) into Eq. (20) taking into account Eq. (15)-Eq. (19) and Eq. (4), we generate the solution of Eq. (3) as:

$$\Psi_{1,3} = \frac{e^{i(-\kappa x+\nu t+\theta)}\left(-B_1\sqrt{\sigma}\,\sin\left(\frac{(\omega_1 t - x(3\kappa\delta+\alpha))\sqrt{\sigma}}{3\kappa\delta+\alpha}\right)+\sigma A_1\right)}{\mu+\cos\left(\frac{(\omega_1 t - x(3\kappa\delta+\alpha))\sqrt{\sigma}}{3\kappa\delta+\alpha}\right)}, \tag{26}$$

$$\Psi_{1,4} = \frac{\left(B_1\sqrt{\sigma}\,\cos\left(\frac{\sqrt{\sigma}(\omega_1 t - x(3\kappa\delta+\alpha))}{3\kappa\delta+\alpha}\right)+\sigma A_1\right)e^{I(-\kappa x+\nu t+\theta)}}{\mu-\sin\left(\frac{\sqrt{\sigma}(\omega_1 t - x(3\kappa\delta+\alpha))}{3\kappa\delta+\alpha}\right)}. \tag{27}$$

4. Sketch and practice of SAEM26 to the perturbed RKL equation

In this section, the main stages of the new extended auxiliary equation method which recently has been introduced in [60] are detailed as follows.

4.1. Sketch of SAEM26 to the perturbed RKL equation

In order to employ the SAEM26 [60], we firstly construct the solutions of Eq. (6) as the following form:

$$\Psi(\eta) = \sum_{l=0}^{M} \Lambda_l \Theta^l(\eta),\ \ \Lambda_M \neq 0, \tag{28}$$

in which Λ_l will be evaluated later, M is the balance number to be computed considering Eq. (6), Eq. (28) and Eq. (29), together. The function $\Theta^l(\eta)$ satisfies the next first order differential equation,

$$(\Theta'(\eta))^2 = \varrho^2\Theta^2(\eta)[1-\chi\Theta^4(\eta)], \tag{29}$$

in which χ, ρ are nonzero values to be figure out later. We can represent the one of the solution for Eq. (29) with the following form:

$$\Theta(\eta) = \mp\sqrt{\frac{2\epsilon}{\sqrt{\chi}\left(e^{2\varrho\eta}+e^{-2\varrho\eta}\right)}} \quad or \quad \Theta(\eta) = \mp\sqrt{\frac{2\epsilon}{\left(e^{2\varrho\eta}+\chi e^{-2\varrho\eta}\right)}},\ \ \epsilon = \mp 1, \tag{30}$$

or in the hyperbolic form:

$$\Theta(\eta) = \mp\sqrt{\frac{\epsilon}{\sqrt{\chi}\cosh(2\varrho\eta)}},\ \ \epsilon = \mp 1. \tag{31}$$

4.2. Practice of SAEM26 to the perturbed RKL equation

With the aid of the homogeneous balance rule considering Eq. (6), Eq. (28) and Eq. (29), $M = 2$ is derived. So, Eq. (28) turns into the following form:

$$\Psi(\eta) = \Lambda_0 + \Lambda_1\Theta(\eta) + \Lambda_2\Theta^2(\eta),\ \ \Lambda_2 \neq 0. \tag{32}$$

When we insert Eq. (32) considering Eq. (29) into Eq. (6), gather all the Θ^l coefficients and equating them to zero, afterwards the following system is generated:

$$\begin{aligned}
&\Theta^0(\eta):\ \left(3\delta^2\kappa^3 + 3\left(\alpha\kappa^2 + \left(\xi\Lambda_0^2+\tau\right)\kappa+\nu\right)\delta + \alpha\Lambda_0^2\xi\right)\Lambda_0 = 0,\\
&\Theta^1(\eta):\ \Lambda_1\left(\left(\kappa^3 - 3\kappa\varrho^2\right)\delta^2 + \left(\alpha\kappa^2 + \left(3\xi\Lambda_0^2+\tau\right)\kappa - \varrho^2\alpha+\nu\right)\delta + \alpha\Lambda_0^2\xi\right) = 0,\\
&\Theta^2(\eta):\ \left(\left(-3\kappa^3+36\kappa\varrho^2\right)\delta^2\left(-9\kappa\xi\Lambda_0^2 - 3\alpha\kappa^2 + 12\varrho^2\alpha - 3\kappa\tau - 3\nu\right)\delta - 3\alpha\Lambda_0^2\xi\right)\Lambda_2\\
&\qquad - 3\Lambda_0\Lambda_1^2(3\delta\kappa+\alpha)\xi = 0,\\
&\Theta^3(\eta):\ \Lambda_1\left(6\Lambda_0\Lambda_2+\Lambda_1^2\right)(3\delta\kappa+\alpha)\xi = 0,\\
&\Theta^4(\eta):\ \left(\Lambda_0\Lambda_2+\Lambda_1^2\right)\Lambda_2(3\delta\kappa+\alpha)\xi = 0,\\
&\Theta^5(\eta):,\Lambda_1\left(3\varrho^2\chi\delta+\Lambda_2^2\xi\right)(3\delta\kappa+\alpha) = 0,\\
&\Theta^6(\eta):\ \left(24\varrho^2\chi\delta+2\Lambda_2^2\xi\right)\Lambda_2(3\delta\kappa+\alpha) = 0.
\end{aligned}$$

Herein, $\xi = 2\gamma + 3\lambda$. After solving the system of equations, we acquire the following solution results:

Result 1:

$$\nu = -\delta\kappa^3 - \alpha\kappa^2 + \left(12\delta\varrho^2-\tau\right)\kappa + 4\varrho^2\alpha,\ \Lambda_0 = 0,\ \Lambda_1 = 0,\ \Lambda_2 = \frac{2\sqrt{-6\xi\chi\delta}\,\varrho}{\xi}. \tag{33}$$

Inserting the parameters in Eq. (33) into Eq. (31) and Eq. (32) taking into account Eq. (4), we derive the following solution of Eq. (3) as:

$$\Psi_{2,1}(x,t) = \frac{4\sqrt{-6\xi\chi\delta}\,\rho\epsilon\,\mathrm{e}^{\mathrm{i}(-\kappa x+\nu t+\theta)}}{\xi\sqrt{\chi}\,\left(\mathrm{e}^{2\rho(x+\omega t)}+\mathrm{e}^{-2\rho(x-\omega t)}\right)}, \tag{34}$$

where ν is as expressed in Eq. (33).

Result 2:

$$\rho = \frac{\Upsilon_2}{2},\ \Lambda_0 = 0,\ \Lambda_1 = 0,\ \Lambda_2 = \frac{\sqrt{6}\,\Upsilon_2\sqrt{-\delta\xi\chi}}{\xi}. \tag{35}$$

where $\Upsilon_2 = \frac{\sqrt{(3\delta\kappa+\alpha)(\delta\kappa^3+\alpha\kappa^2+\kappa\tau+\nu)}}{(3\delta\kappa+\alpha)}$. Inserting the parameters in Eq. (35) into Eq. (31) and Eq. (32) taking into account Eq. (4), we produce the following solution of Eq. (3) as:

$$\Psi_{2,2}(x,t) = \frac{2\Upsilon_2\sqrt{-6\chi\delta\xi}\,\epsilon\,\mathrm{e}^{-\mathrm{i}(\kappa x-\nu t-\theta)+\Upsilon_2\frac{\left(8\delta^2\kappa^3+\left(8\alpha\kappa^2+2\kappa\tau-\nu\right)\delta+\alpha(2\alpha\kappa+\tau)\right)t+x(3\delta\kappa+\alpha)}{(3\delta\kappa+\alpha)}}}{\sqrt{\chi}\,\xi\left(\mathrm{e}^{-\frac{2\Upsilon_2\left(\left(-8\delta^2\kappa^3+\left(-8\alpha\kappa^2-2\kappa\tau+\nu\right)\delta-2\alpha^2\kappa-\alpha\tau\right)t-x(3\delta\kappa+\alpha)\right)}{(3\delta\kappa+\alpha)}}+1\right)}. \tag{36}$$

5. Sketch and practice of the UREEM to the perturbed RKL equation

In this section, the main stages of the UREEM [56] are explained.

5.1. Sketch of the UREEM to the perturbed RKL equation

Presume that Eq. (6) has a solution of the form:

$$\Psi(\eta) = \sum_{l=0}^{N}\Lambda_l\Theta^l(\eta),\ \ \lambda_N \neq 0 \tag{37}$$

in which Λ_l are real values to be computed. The function $\Theta(\eta)$ fulfills the next first order differential equation,

$$\Theta'(\eta) = \rho_0 + \rho_2\Theta(\eta) + \rho_2\Theta^2(\eta). \tag{38}$$

The Eq. (38) has its special solutions as the following:

Set 1: If $\Delta > 0$, then,

$$\Theta_1 = -\frac{\rho_1}{2\rho_2} - \frac{\sqrt{\Delta}}{2\rho_2}\tanh\left(\frac{\sqrt{\Delta}}{2}\eta\right),$$

$$\Theta_2 = -\frac{\rho_1}{2\rho_2} - \frac{\sqrt{\Delta}}{2\rho_2}\coth\left(\frac{\sqrt{\Delta}}{2}\eta\right).$$

Set 2: If $\Delta = 0$, then,

$$\Theta_3 = -\frac{\rho_1}{2\rho_2} - \frac{1}{\rho_2\eta + C}.$$

Set 3: If $\Delta < 0$, then,

$$\Theta_4 = -\frac{\rho_1}{2\rho_2} - \frac{\sqrt{-\Delta}}{2\rho_2}\tan\left(\frac{\sqrt{-\Delta}}{2}\eta\right),$$

$$\Theta_5 = -\frac{\rho_1}{2\rho_2} - \frac{\sqrt{-\Delta}}{2\rho_2}\cot\left(\frac{\sqrt{-\Delta}}{2}\eta\right).$$

in which $\Delta = \rho_1^2 - 4\rho_0\rho_2$ and C is an arbitrary constant. Despite Eq. (38) has twenty-seven solutions expressed in many researches [63–65], these solutions are equivalent to the above solutions.

5.2. Practice of the UREEM to the perturbed RKL equation

With the help of the homogeneous balance rule by considering the terms $\Psi''(\eta)$ and $\Psi^3(\eta)$ in Eq. (6), $M = 1$ is achieved. Hence, Eq. (37) turns into the following form:

$$\Psi(\eta) = \Lambda_0 + \Lambda_1\Theta(\eta),\ \ \Lambda_1 \neq 0. \tag{39}$$

Insert Eq. (39) and its derivatives regarding Eq. (38) into Eq. (6), then we acquire the polynomial in powers of $\Theta(\eta)$. Compiling all the Θ^l coefficients and considering the coefficients as zero, then the following algebraic system is resulted:

$$\begin{aligned}
&\Theta^0(\eta):\ -3\delta\left(\delta\kappa^3+\alpha\kappa^2+\kappa\tau+\nu\right)\Lambda_0-(3\kappa\delta+\alpha)\xi\Lambda_0^3+3\delta(3\kappa\delta+\alpha)\Lambda_1\rho_0\rho_1=0,\\
&\Theta^1(\eta):\ -\delta\left(\delta\kappa^3+\alpha\kappa^2+\kappa\tau+\nu\right)\Lambda_1-(3\kappa\delta+\alpha)\xi\Lambda_0^2\Lambda_1+2\delta(3\kappa\delta+\alpha)\Lambda_1\rho_0\rho_2+\delta(3\kappa\delta+\alpha)\Lambda_1\rho_1^2=0,\\
&\Theta^2(\eta):\ \left(-\Lambda_0\xi\Lambda_1+3\rho_1\rho_2\delta\right)(3\kappa\delta+\alpha)\Lambda_1=0,\\
&\Theta^3(\eta):\ -(3\kappa\delta+\alpha)\xi\Lambda_1^3+6\delta(3\kappa\delta+\alpha)\Lambda_1\rho_2^2=0.
\end{aligned}$$

where $\xi=2\gamma+3\lambda$. Solving the system above, the following solution sets are derived:

Result 1:

$$\rho_1=\frac{\sqrt{6\xi\delta}\,Y_3}{3\delta},\ \Lambda_0=Y_3,\ \Lambda_1=\frac{\sqrt{6}\sqrt{\xi\delta}\,\rho_2}{\xi}, \tag{40}$$

where $Y_3=\frac{\sqrt{-3\xi\delta(3\delta\kappa+\alpha)(\delta\kappa^3-6\delta\kappa\rho_0\rho_2+\alpha\kappa^2-2\alpha\rho_0\rho_2+\kappa\tau+\nu)}}{(3\delta\kappa+\alpha)\xi}$.

Inserting the parameters in Eq. (40) into Eq. (31) and Eq. (32) taking into account Eq. (4), we derive the following solutions of Eq. (3) as:

$$\Psi_{3,1}(x,t)=\frac{e^{i(-\kappa x+\nu t+\theta)}\tanh\left(\frac{(\omega_2 t-x(3\kappa\delta+\alpha))Y_3}{6\kappa\delta+2\alpha}\right)\sqrt{6\xi\delta}\,Y_4}{2\xi}, \tag{41}$$

$$\Psi_{3,2}(x,t)=\frac{e^{i(-\kappa x+\nu t+\theta)}\coth\left(\frac{(\omega_2 t-x(3\kappa\delta+\alpha))Y_4}{6\kappa\delta+2\alpha}\right)\sqrt{6\xi\delta}\,Y_4}{2\xi}, \tag{42}$$

$$\Psi_{3,3}(x,t)=-\frac{e^{i(-\kappa x+\nu t+\theta)}\,Y_5\tan\left(\frac{\sqrt{2}(\omega_2 t-x(3\kappa\delta+\alpha))}{6\kappa\delta+2\alpha}Y_5\right)\sqrt{3\xi\delta}}{\xi}, \tag{43}$$

$$\Psi_{3,4}(x,t)=-\frac{e^{i(-\kappa x+\nu t+\theta)}\,Y_5\cot\left(\frac{\sqrt{2}(\omega_2 t-x(3\kappa\delta+\alpha))}{6\kappa\delta+2\alpha}Y_5\right)\sqrt{3\xi\delta}}{\xi}, \tag{44}$$

where $\omega_2=\left(-8\delta^2\kappa^3-8\alpha\delta\kappa^2+\left(-2\alpha^2-2\delta\tau\right)\kappa+\delta\nu-\alpha\tau\right)$, $Y_4=\sqrt{\frac{-2\delta\kappa^3-2\alpha\kappa^2-2\kappa\tau-2\nu}{3\kappa\delta+\alpha}}$ and $Y_5=\sqrt{\frac{\delta\kappa^3+\alpha\kappa^2+\kappa\tau+\nu}{3\kappa\delta+\alpha}}$.

6. Results and discussion

In this section, the graphical portraits of some solution functions are given. These illustrations both demonstrate the soliton graphs of some solutions and involve the graphs which examine the effects of the presented model's parameters on soliton dynamics. Selecting suitable variables of unknown parameters in the obtained solutions, we depict different graphs with 3D, contour and 2D plots.

In Fig. 1a and 1b, we demonstrate the 3D and contour graphs of $|\Psi_{1,1}(x,t)|^2$ in Eq. (22) for $\lambda=1.5,\gamma=1,\alpha=1,\delta=2,\kappa=0.25,\tau=-2,\nu=-0.75,\mu=2$, and $\theta=1$. Besides, 2D visualization at t = 3,5,7 is displayed in Fig. 1c. We can interpret from Fig. 1c that the soliton goes to the right as t increases. Fig. 1a and 1c show the dark soliton type of $|\Psi_{1,1}(x,t)|^2$. Fig. 1d, 1e and 1f represent the 3D, contour and 2D portraits for the real part of $\Psi_{1,1}(x,t)$.

In Fig. 2a and 2b, we exhibit the 3D and contour graphs of $|\Psi_{2,1}(x,t)|^2$ in Eq. (34) for $\lambda=1.5,\gamma=1,\alpha=3,\chi=1,\delta=2,\kappa=-1,\tau=-2,\nu=-2,\varrho=-0.5,\theta=10$, and $\epsilon=1$. 2D visualization at t = 3,5,7 is also displayed in Fig. 2c. We can understand from Fig. 2c that the soliton goes to the left as t decreases. Fig. 2a and 2c show the bright soliton type of $|\Psi_{2,1}(x,t)|^2$. In Fig. 3, we examine that how the parameters τ,λ,γ, and δ in the perturbed RKL model have an effect on soliton behavior. Fig. 3a shows the effect of the parameter τ, which indicates the inter-modal dispersion, for the values $-3,-2,-1,3,2,1$, respectively. We can say from Fig. 3a that if $\tau<0$ and increasing, the soliton goes to the left. If $\tau>0$ and decreasing, the soliton moves to the right. In addition, in both cases, there is no change in the vertical amplitude of the soliton and the skirts of the soliton stay on the same horizontal axis. Fig. 3b represents the role of the parameter λ, which specifies the coefficient of the self-steepening for short pulses, for the values $-3,-2,-1,3,2,1$, respectively. For $\lambda<0$, the soliton's height increases as λ increases. For $\lambda>0$, the soliton's height decreases as λ increases. Although the position of the peak of the soliton changes vertically, in both cases there is no change in the horizontal position of the soliton; in other words, the soliton remains symmetrical with respect to a vertical axis passing through the peak. Fig. 3c represents the impact of the parameter γ, which describes the coefficient of the higher-order dispersion, for the values $-3,-2,-1,3,2,1$, respectively. Even if we obtain a graph in Fig. 3b similar to the previous one in Fig. 3c, we cannot say that the effect of the γ is exactly the same as in the previous one. Because although the soliton appears symmetrical with respect to the vertical axis passing through the peak, its skirts stay on the same horizontal axis, and the position of the soliton's peak changes according to different γ values, in the case of $\gamma<0$ and increasing, the vertical amplitude of the soliton decreases for -3 and -1 values. For $\gamma=-2$, we see that this effect occurs as an increase in the vertical amplitude of the soliton. Moreover, the amplitude formed for $\gamma=-2$ is a situation in which the amplitude of the soliton is maximally formed among all the γ values examined. We can explain this situation for $\gamma=-2$ as the difficulty of controlling both the nonlinear parameters and their interaction with other parameters. When $\gamma>0$ and increasing, the

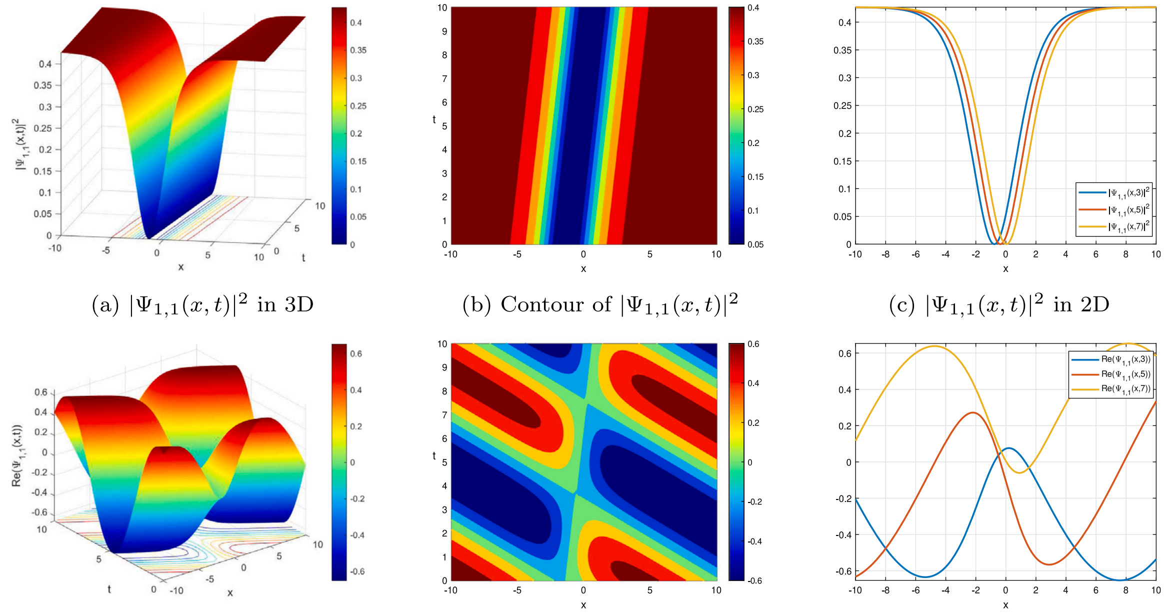

(a) $|\Psi_{1,1}(x,t)|^2$ in 3D (b) Contour of $|\Psi_{1,1}(x,t)|^2$ (c) $|\Psi_{1,1}(x,t)|^2$ in 2D

(d) $Re(\Psi_{1,1}(x,t))$ in 3D (e) Contour of $Re(\Psi_{1,1}(x,t))$ (f) $Re(\Psi_{1,1}(x,t))$ in 2D

Fig. 1. Some plots of $\Psi_{1,1}(x,t)$ in Eq. (22) for $\lambda = 1.5, \gamma = 1, \alpha = 1, \delta = 2, \kappa = 0.25, \tau = -2, \nu = -0.75, \mu = 2, \theta = 1$.

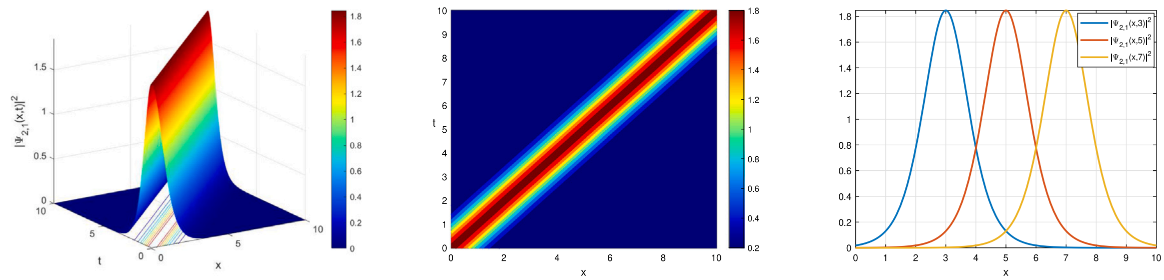

(a) $|\Psi_{2,1}(x,t)|^2$ in 3D (b) Contour of $|\Psi_{2,1}(x,t)|^2$ (c) $|\Psi_{2,1}(x,t)|^2$ in 2D

Fig. 2. Some views of $\Psi_{2,1}(x,t)$ in Eq. (34) for $\lambda = 1.5, \gamma = 1, \alpha = 3, \chi = 1, \delta = 2, \kappa = -1, \tau = -2, \nu = -2, \varrho = -0.5, \theta = 10$, and $\epsilon = 1$.

amplitude of the soliton decreases. Fig. 3d expresses the impact of the parameter δ, which is the third-order dispersion (TOD) term, for the values $-1.5, -1.75, -2, 1.5, 1.75, 2$, respectively. While $\delta < 0$ and increasing, the soliton goes to the left and the soliton's height decreases. When $\delta > 0$ and increasing, the soliton goes to the left and the soliton's height increase. As can be seen from Fig. 3d that, when the absolute values of δ parameter are the same (positive or negative), the vertical amplitude of the soliton becomes the same, only a decrease (when negative) or increase (when positive) and left movement (increase) are observed in the amplitude of the soliton.

In Fig. 4a and 4b, we indicate the 3D and contour graphs of $|\Psi_{3,1}(x,t)|^2$ in Eq. (41) for $\alpha = -1$, $\tau = 1.5$, $\lambda = -3$, $\gamma = 1.5$, $\delta = -1$, $\theta = 10$, $\kappa = 0.5$, $\nu = 1.5$, $\rho_0 = 1$, $\rho_2 = 0.5$. 2D visualization at $t = 3, 5, 7$ is also displayed in Fig. 4c. We can say from Fig. 4c that the soliton goes to the right as t increases. Fig. 4a and 4c show the dark soliton type of $|\Psi_{3,1}(x,t)|^2$. In Fig. 5, we examine that how the parameters τ, λ, γ, and δ in the perturbed RKL equation have an effect on soliton dynamics. Fig. 5a shows the effect of the parameter τ for the values $-1.75, -1.5, -1, 1.75, 1.5, 1$, respectively. We can say that if $\tau < 0$ and increasing, the soliton's height increases and the soliton's peak goes to the right on the horizontal axis. If $\tau > 0$ and decreasing, the soliton's height decreases and the soliton's peak also goes to the right on the horizontal axis. In addition, we can say from Fig. 5a that the horizontal amplitude of the soliton (solid lines) when $\tau < 0$ is larger than when $\tau > 0$ (dashed lines). Fig. 5b represents the role of the parameter λ for the values $-3, -2.25, -1.5, 3, 2.25, 1.5$, respectively. For $\lambda < 0$ and increases, the soliton's height increases. For $\lambda > 0$ and decreases, the soliton's height increases. Fig. 5c represents the impact of the parameter γ for the values $-3, -2, -1, 3, 2, 1$, respectively. Although the graph of Fig. 5c is similar in shape to the graph of Fig. 5b, it has differences in terms of parameter effect. That is: when γ is both negative and positive, the vertical amplitude of the soliton increases depending on the increase in γ, and this increase occurs more when γ is negative than when γ is positive. The soliton again remains symmetrical with respect to the vertical axis passing

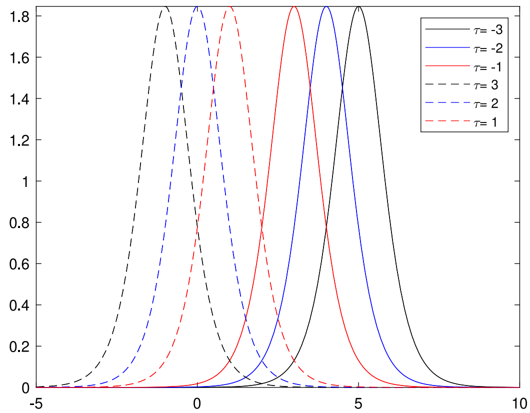

(a) 2D plot of $|\Psi_{2,1}(x,t)|^2$ for diverse τ

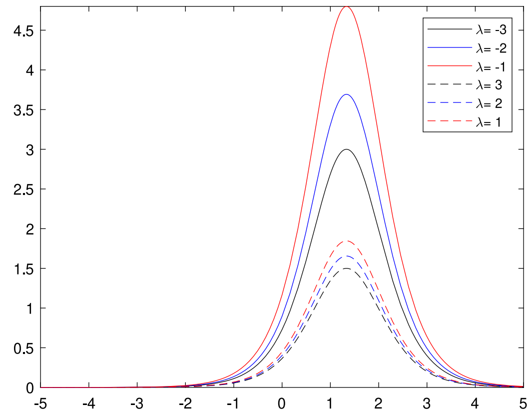

(b) 2D plot of $|\Psi_{2,1}(x,t)|^2$ for diverse λ

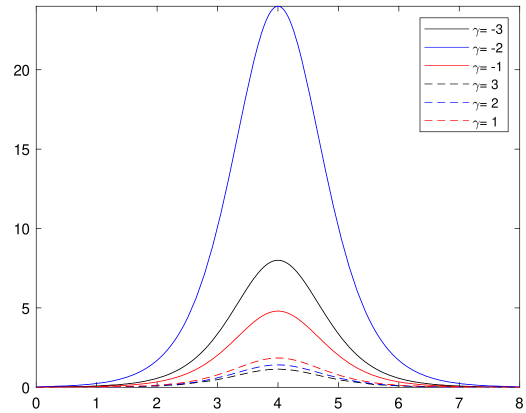

(c) 2D plot of $|\Psi_{2,1}(x,t)|^2$ for diverse γ

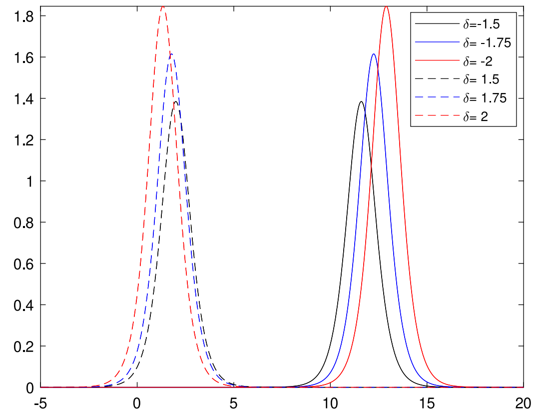

(d) 2D plot of $|\Psi_{2,1}(x,t)|^2$ for diverse δ

Fig. 3. The different silhouettes of $\Psi_{2,1}(x,t)$ in Eq. (34) for $\alpha = 3, \chi = 1, \kappa = -1, \nu = -2, \rho = -0.5, \theta = 10$, and $\epsilon = 1$.

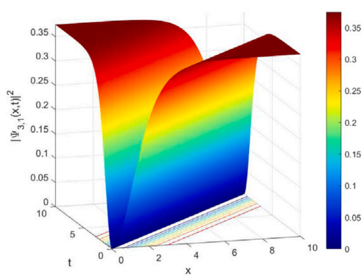

(a) $|\Psi_{3,1}(x,t)|^2$ in 3D

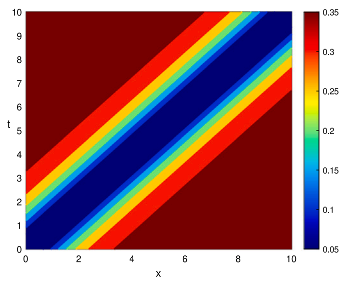

(b) Contour of $|\Psi_{3,1}(x,t)|^2$

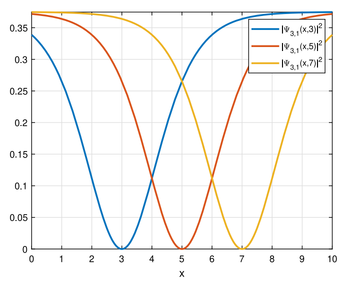

(c) $|\Psi_{3,1}(x,t)|^2$ in 2D

Fig. 4. Various plots of $\Psi_{3,1}(x,t)$ in Eq. (41) for $\alpha = -1, \tau = 1.5, \lambda = -3, \gamma = 1.5, \delta = -1, \theta = 10, \kappa = 0.5, \nu = 1.5, \rho_0 = 1, \rho_2 = 0.5$.

through its peak. Fig. 5d expresses the impact of the parameter δ for the values $-1, -2, -3$, respectively. As $\delta < 0$ and increases, the soliton moves to the left and the soliton's height decreases. Here, although the amount of increase in δ from -3 to -2 (red to blue) is equal to the amount of increase from -2 to -1 (blue to black), the vertical distance between the skirts of the soliton is not proportional, we see that this drop is especially more dramatic for $\delta = -1$ (black line). We can explain this issue with the control difficulty of the situations arising from the interaction of the mentioned parameters both with themselves and with other nonlinear terms, and the reflection of this difficulty on the soliton behavior.

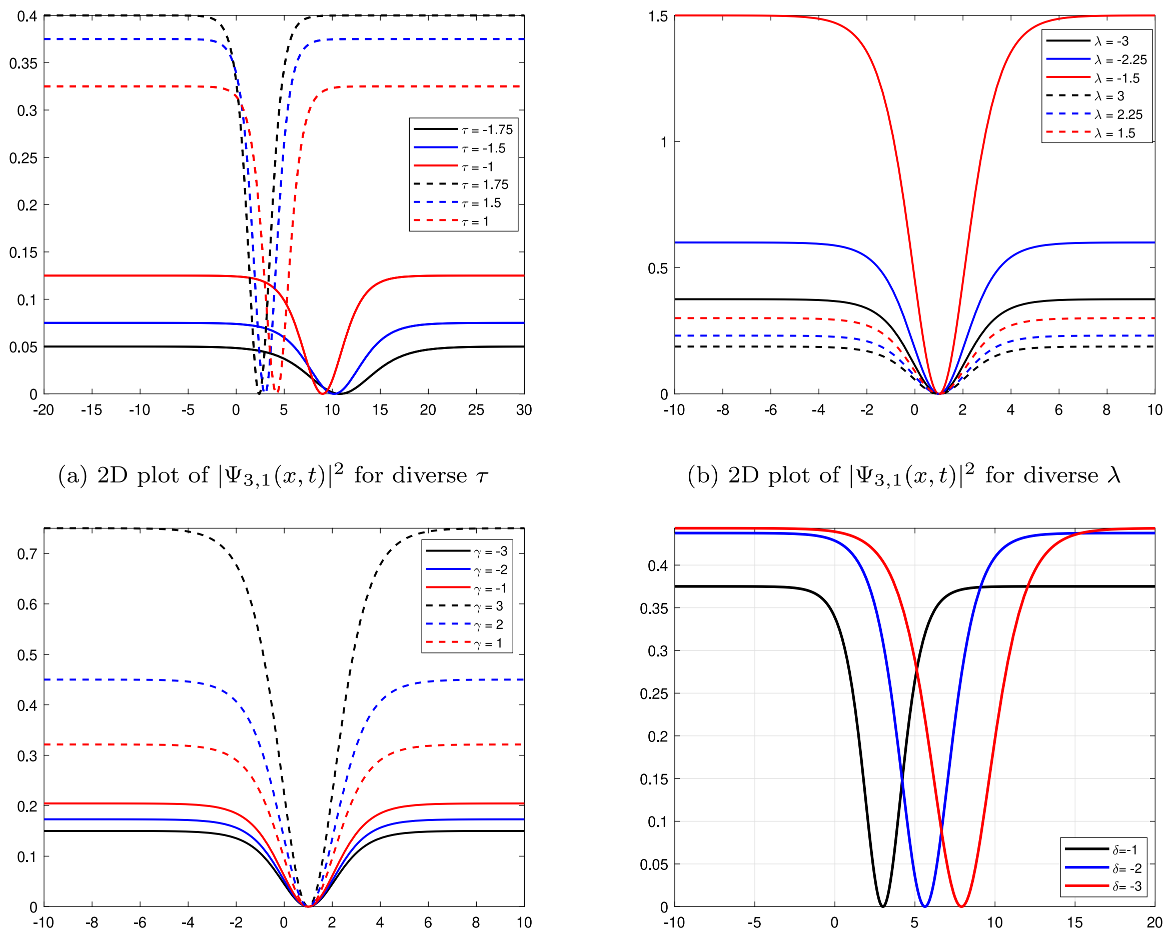

(a) 2D plot of $|\Psi_{3,1}(x,t)|^2$ for diverse τ

(b) 2D plot of $|\Psi_{3,1}(x,t)|^2$ for diverse λ

(c) 2D plot of $|\Psi_{3,1}(x,t)|^2$ for diverse γ

(d) 2D plot of $|\Psi_{3,1}(x,t)|^2$ for diverse δ

Fig. 5. The various portraits of $\Psi_{3,1}(x,t)$ in Eq. (41) for $\alpha = -1, \theta = 10, \kappa = 0.5, \nu = 1.5, \rho_0 = 1$, and $\rho_2 = 0.5$. (For interpretation of the references to color in this figure legend, the reader is referred to the web version of this article.)

In Fig. 6a and 6b, the 3D and contour graphs of $|\Psi_{3,3}(x,t)|^2$ in Eq. (34) for $\alpha = 1.5$, $\tau = 2$, $\gamma = 1.5$, $\lambda = 2$, $\delta = 2$, $\kappa = -0.5$, $\nu = -0.5781$, $\theta = 10$, $\rho_0 = 0.5$, and $\rho_2 = 1$ are displayed. 2D visualization at $t = 3, 5, 7$ is also demonstrated in Fig. 6c. We can see from Fig. 6c that the soliton goes to the left as t increases. Fig. 6a and 6c show the singular soliton type of $|\Psi_{3,3}(x,t)|^2$. In Fig. 7, we show that how the parameters τ, λ, γ, and δ in the perturbed RKL equation have an effect on soliton behavior. Fig. 7a shows the effect of the parameter τ for the values $-0.5, -0.4, -0.3, 0.5, 0.4, 0.3$, respectively. We can say that if $\tau < 0$ and increasing, the soliton goes to the left on the horizontal axis (solid lines). When $\tau > 0$ and increasing, the soliton also moves to the left on the horizontal axis. Fig. 7b represents the role of the parameter λ for the values $-3, -2.25, -1.5, 3, 2.25, 1.5$, respectively. For $\lambda < 0$ and increases, the skirts of the soliton remain on the horizontal axis and the horizontal distance between the skirts of the soliton increases. While $\lambda > 0$ and increases, the inverse effect is observed as in the previous situation. Fig. 7c represents the impact of the parameter γ for the values $-1.5, -1, -0.5, 1.5, 1, 0.5$. According to Fig. 7b for $\gamma < 0$, the amount of horizontal decrease between the skirts of the soliton is realized with smaller reduction amounts in Fig. 7c. At the same time, the height of the soliton is higher than Fig. 7b. Fig. 7d expresses the impact of the parameter δ for the values $-1.5, -1, -0.5, 1.5, 1, 0.5$. As δ is negative or positive and increasing, the soliton moves to the left.

7. Conclusion

In this study, the GPREM, SAEM26, and UREEM as powerful mathematical tools have been implemented to derive the soliton solutions of the perturbed RKL equation. Various soliton solutions have also been acquired. These solutions include various wave structures, such as singular, bright, and dark solitons. 3D, contour and 2D graphics of the obtained soliton solutions have been demonstrated. Moreover, the effects of the model parameters on soliton dynamics are for the first time examined. It is also shown

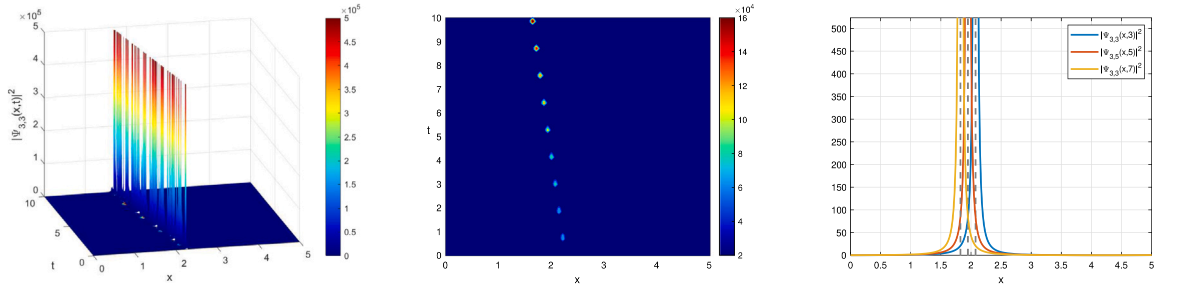

(a) $|\Psi_{3,3}(x,t)|^2$ in 3D (b) Contour of $|\Psi_{3,3}(x,t)|^2$ (c) $|\Psi_{3,3}(x,t)|^2$ in 2D

Fig. 6. The plots of $\Psi_{3,3}(x,t)$ in Eq. (43): (a) the 3D graph of the square of modulus, (b) the contour graph of the square of modulus, (c) the 2D graph of the square of modulus for $\alpha = 1.5, \tau = 2, \gamma = 1.5, \lambda = 2\delta = 2, \kappa = -0.5, \nu = -0.5781, \theta = 10, \rho_0 = 0.5$, and $\rho_2 = 1$.

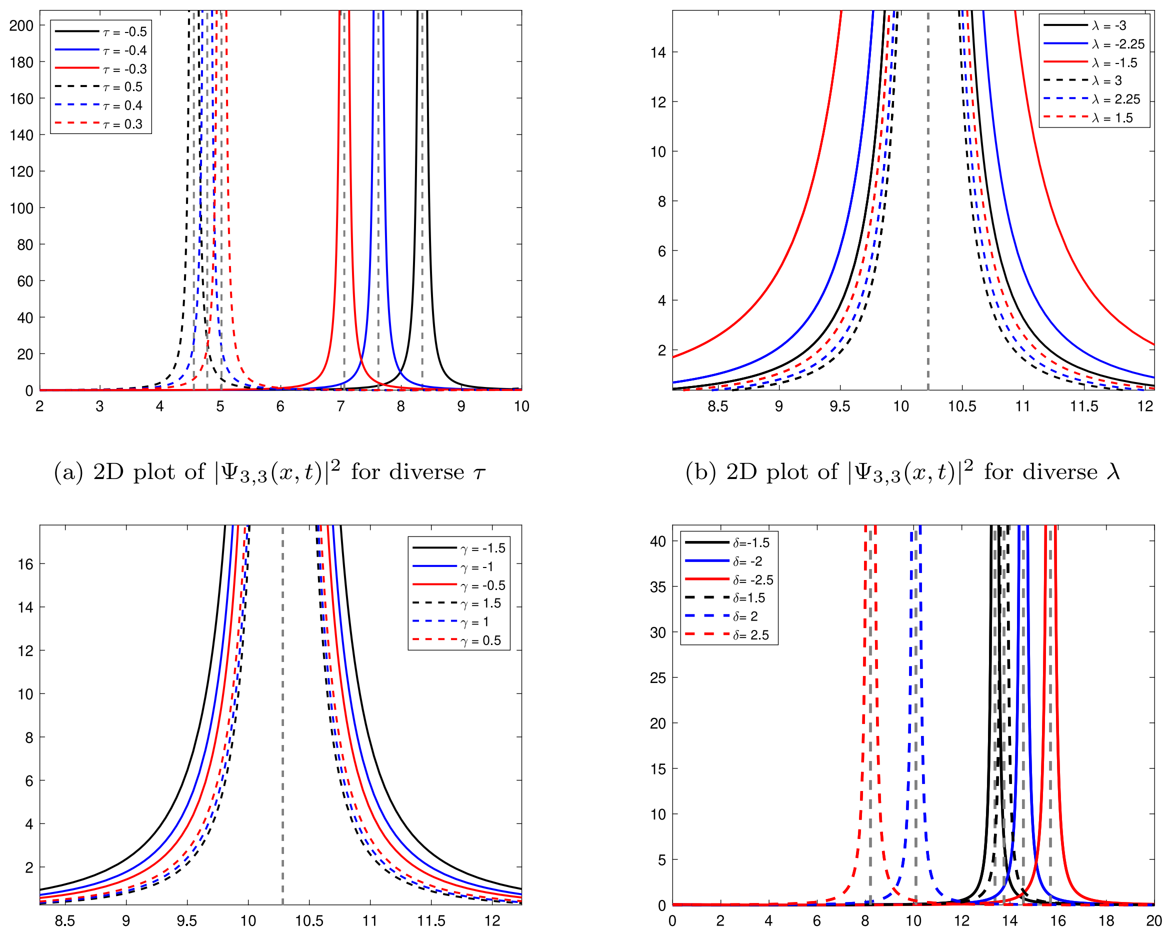

(a) 2D plot of $|\Psi_{3,3}(x,t)|^2$ for diverse τ

(b) 2D plot of $|\Psi_{3,3}(x,t)|^2$ for diverse λ

(c) 2D plot of $|\Psi_{3,3}(x,t)|^2$ for diverse γ

(d) 2D plot of $|\Psi_{3,3}(x,t)|^2$ for diverse δ

Fig. 7. The various portraits of $\Psi_{3,3}(x,t)$ in equation Eq. (43) for $\alpha = 1.5, \kappa = -0.5, \nu = -0.5781, \theta = 10, \rho_0 = 0.5$, and $\rho_2 = 1$.

how the parameters τ, λ, γ, and δ in the perturbed RKL model have an effect on soliton dynamics. As a result of the study, this study includes a number of complexities and difficulties, both due to the definition and limitations of the problem, and to the interaction of the parameters themselves and other nonlinear terms. In this sense, long trials were made for parameter selection to obtain the soliton types obtained in the study and to preserve the shape of these solitons in order to examine the parameter effect. Therefore, in such problems, the determination of the parameters in question and the preservation of the obtained soliton involve a series of difficulties. It has also been shown in this study that the effects of such parameters on different soliton types can be different. The presented graphics will help to understand the physical properties and dynamical behavior of the perturbed RKL equation. It can be concluded that soliton solutions of a large family of nonlinear physics models can be productively constructed utilizing the proposed methods. It can be said that GPREM, SAEM26, and UREEM will be very profitable approaches for researchers. So, the GPREM, SAEM26, and UREEM can be successfully employed to acquire successful results when analyzing and investigating soliton solutions of different nonlinear fractional complex models.

Declaration of competing interest

The authors declare that they have no known competing financial interests or personal relationships that could have appeared to influence the work reported in this paper.

Data availability

No data was used for the research described in the article.

References

[1] W. Liu, Y. Zhang, Z. Luan, Q. Zhou, M. Mirzazadeh, M. Ekici, A. Biswas, Dromion-like soliton interactions for nonlinear Schrödinger equation with variable coefficients in inhomogeneous optical fibers, Nonlinear Dynam. 96 (1) (2019) 729–736.
[2] M. Ekici, M. Mirzazadeh, A. Sonmezoglu, Q. Zhou, H. Triki, M.Z. Ullah, S.P. Moshokoa, A. Biswas, Optical solitons in birefringent fibers with Kerr nonlinearity by exp-function method, Optik 131 (2017) 964–976.
[3] M. Mirzazadeh, M. Ekici, Q. Zhou, A. Biswas, Exact solitons to generalized resonant dispersive nonlinear Schrödinger's equation with power law nonlinearity, Optik 130 (2017) 178–183.
[4] A. Bansal, A. Biswas, Q. Zhou, M. Babatin, Lie symmetry analysis for cubic–quartic nonlinear Schrödinger's equation, Optik 169 (2018) 12–15.
[5] Y. Yıldırım, A. Biswas, S. Khan, M.F. Mahmood, H.M. Alshehri, Highly dispersive optical soliton perturbation with Kudryashov's sextic-power law of nonlinear refractive index, Ukrainian J. Phys. Opt. 23 (1) (2022).
[6] E. Zayed, R. Shohib, M. Alngar, A. Biswas, M. Ekici, S. Khan, A. Alzahrani, M. Belic, Optical solitons and conservation laws associated with Kudryashov's sextic power-law nonlinearity of refractive index, Ukrainian J. Phys. Opt. 22 (1) (2021).
[7] A.J.M. Jawad, M.D. Petković, A. Biswas, Modified simple equation method for nonlinear evolution equations, Appl. Math. Comput. 217 (2) (2010) 869–877.
[8] E.M. Zayed, A note on the modified simple equation method applied to Sharma–Tasso–Olver equation, Appl. Math. Comput. 218 (7) (2011) 3962–3964.
[9] M.M. Khater, The modified simple equation method and its applications in mathematical physics and biology, Glob. J. Sci. Front. Res. 15 (4) (2015) 1–19.
[10] K.K. Ali, A.M. Wazwaz, M. Osman, Optical soliton solutions to the generalized nonautonomous nonlinear Schrödinger equations in optical fibers via the sine-Gordon expansion method, Optik 208 (2020) 164132.
[11] S.N. Ananna, T. An, M. Asaduzzaman, M.S. Rana, et al., Sine-Gordon expansion method to construct the solitary wave solutions of a family of 3D fractional WBBM equations, Results Phys. 40 (2022) 105845.
[12] M.R.A. Fahim, P.R. Kundu, M.E. Islam, M.A. Akbar, M. Osman, Wave profile analysis of a couple of $(3+1)$-dimensional nonlinear evolution equations by sine-Gordon expansion approach, J. Ocean Eng. Sci. 7 (3) (2022) 272–279.
[13] A. Biswas, H. Rezazadeh, M. Mirzazadeh, M. Eslami, M. Ekici, Q. Zhou, S.P. Moshokoa, M. Belic, Optical soliton perturbation with Fokas–Lenells equation using three exotic and efficient integration schemes, Optik 165 (2018) 288–294.
[14] Y. Yıldırım, A. Biswas, P. Guggilla, S. Khan, H.M. Alshehri, M.R. Belic, Optical solitons in fibre bragg gratings with third-and fourth-order dispersive reflectivities, Ukrainian J. Phys. Opt. 22 (4) (2021) 239–254.
[15] Y. Yildrim, A. Biswas, A. Dakova, P. Guggilla, S. Khan, H.M. Alshehri, M.R. Belic, Cubic–quartic optical solitons having quadratic–cubic nonlinearity by sine–Gordon equation approach, Ukrainian J. Phys. Opt. 22 (4) (2021).
[16] M. Kabir, A. Khajeh, E. Abdi Aghdam, A. Yousefi Koma, Modified kudryashov method for finding exact solitary wave solutions of higher-order nonlinear equations, Math. Methods Appl. Sci. 34 (2) (2011) 213–219.
[17] D. Kumar, M. Kaplan, Application of the modified kudryashov method to the generalized Schrödinger–Boussinesq equations, Opt. Quantum Electron. 50 (9) (2018) 1–14.
[18] M. Abdou, Further improved F-expansion and new exact solutions for nonlinear evolution equations, Nonlinear Dynam. 52 (3) (2008) 277–288.
[19] M.S. Islam, K. Khan, M.A. Akbar, Application of the improved F-expansion method with riccati equation to find the exact solution of the nonlinear evolution equations, J. Egyptian Math. Soc. 25 (1) (2017) 13–18.
[20] Y. Yıldırım, A. Biswas, A.J.M. Jawad, M. Ekici, Q. Zhou, S. Khan, A.K. Alzahrani, M.R. Belic, Cubic-quartic optical solitons in birefringent fibers with four forms of nonlinear refractive index by exp-function expansion, Results Phys. 16 (2020) 102913.
[21] M. Ozisik, On the optical soliton solution of the $(1+1)$- dimensional perturbed NLSE in optical nano-fibers, Optik 250 (2022) 168233.
[22] M. Ozisik, Novel $(2+1)$ and $(3+1)$ forms of the biswas-milovic equation and optical soliton solutions via two efficient techniques, Optik (2022) 169798.
[23] H. Esen, N. Ozdemir, A. Secer, M. Bayram, Traveling wave structures of some fourth-order nonlinear partial differential equations, J. Ocean Eng. Sci. (2021).
[24] A. Tripathy, S. Sahoo, S.S. Ray, M. Abdou, New optical soliton solutions of Biswas–Arshed model with Kerr law nonlinearity, Internat. J. Modern Phys. B 35 (26) (2021) 2150263.
[25] F. Tascan, A. Bekir, M. Koparan, Travelling wave solutions of nonlinear evolution equations by using the first integral method, Commun. Nonlinear Sci. Numer. Simul. 14 (5) (2009) 1810–1815.
[26] N. Taghizadeh, M. Mirzazadeh, A.S. Paghaleh, Exact solutions of some nonlinear evolution equations via the first integral method, Ain Shams Eng. J. 4 (3) (2013) 493–499.
[27] A. Ghosh, S. Maitra, The first integral method and some nonlinear models, Comput. Appl. Math. 40 (3) (2021) 1–16.
[28] M. Ozisik, M. Cinar, A. Secer, M. Bayram, Optical solitons with Kudryashov's sextic power-law nonlinearity, Optik 261 (2022) 169202.
[29] X. Liu, W. Liu, H. Triki, Q. Zhou, A. Biswas, Periodic attenuating oscillation between soliton interactions for higher-order variable coefficient nonlinear Schrödinger equation, Nonlinear Dynam. 96 (2) (2019) 801–809.
[30] A. Biswas, M. Ekici, A. Sonmezoglu, M.R. Belic, Highly dispersive optical solitons with cubic-quintic-septic law by F-expansion, Optik 182 (2019) 897–906.
[31] O. Gonzalez-Gaxiola, A. Biswas, Y. Yıldırım, H.M. Alshehri, Highly dispersive optical solitons in birefringent fibres with non-local form of nonlinear refractive index: Laplace–Adomian decomposition, Ukrainian J. Phys. Opt. 23 (2) (2022) 68–76.

[32] H. Esen, N. Ozdemir, A. Secer, M. Bayram, On solitary wave solutions for the perturbed Chen–Lee–Liu equation via an analytical approach, Optik 245 (2021) 167641.
[33] I. Onder, A. Secer, M. Ozisik, M. Bayram, On the optical soliton solutions of Kundu–Mukherjee–Naskar equation via two different analytical methods, Optik 257 (2022) 168761.
[34] M. Ekici, A. Sonmezoglu, A. Biswas, M.R. Belic, Optical solitons in (2+ 1)–dimensions with Kundu–Mukherjee–Naskar equation by extended trial function scheme, Chinese J. Phys. 57 (2019) 72–77.
[35] M. Ekici, M. Mirzazadeh, A. Sonmezoglu, Q. Zhou, S.P. Moshokoa, A. Biswas, M. Belic, Dark and singular optical solitons with Kundu–Eckhaus equation by extended trial equation method and extended G'/G-expansion scheme, Optik 127 (22) (2016) 10490–10497.
[36] N. Ozdemir, A. Secer, M. Ozisik, M. Bayram, Perturbation of dispersive optical solitons with Schrödinger–Hirota equation with Kerr law and spatio-temporal dispersion, Optik 265 (2022) 169545.
[37] A. Biswas, Y. Yildirim, E. Yasar, Q. Zhou, S.P. Moshokoa, M. Belic, Optical solitons for Lakshmanan–Porsezian–Daniel model by modified simple equation method, Optik 160 (2018) 24–32.
[38] A.R. Adem, B.P. Ntsime, A. Biswas, S. Khan, A.K. Alzahrani, M.R. Belic, Stationary optical solitons with nonlinear chromatic dispersion for Lakshmanan–Porsezian–Daniel model having Kerr law of nonlinear refractive index, Ukrainian J. Phys. Opt. 22 (2) (2021) 83–86.
[39] A. Biswas, J. Edoki, P. Guggilla, S. Khan, A.K. Alzahrani, M.R. Belic, Cubic-quartic optical soliton perturbation with Lakshmanan-Porsezian-Daniel model by semi-inverse variational principle, Ukrainian J. Phys. Opt. 22 (2021) 123.
[40] A. Al Qarni, A. Bodaqah, A. Mohammed, A. Alshaery, H. Bakodah, A. Biswas, Cubic-quartic optical solitons for Lakshmanan-Porsezian-Daniel equation by the improved adomian decomposition scheme, Ukrainian J. Phys. Opt. 23 (4) (2022) 228–242.
[41] M. Ozisik, A. Secer, M. Bayram, The bell-shaped perturbed dispersive optical solitons of Biswas–Arshed equation using the new Kudryashov's approach, Optik 267 (2022) 169650.
[42] M. Ozisik, A. Secer, M. Bayram, On the examination of optical soliton pulses of Manakov system with auxiliary equation technique, Optik (2022) 169800.
[43] F. Sun, Optical solutions of Sasa-Satsuma equation in optical fibers, Optik 228 (2021) 166127.
[44] E.M. Zayed, R. Shohib, M.E. Alngar, A. Biswas, Y. Yıldırım, A. Dakova, H.M. Alshehri, M.R. Belic, Optical solitons in the Sasa-Satsuma model with multiplicative noise via Itô calculus, Ukrainian J. Phys. Opt. 23 (1) (2022).
[45] R. Radhakrishnan, A. Kundu, M. Lakshmanan, Coupled nonlinear Schrödinger equations with cubic-quintic nonlinearity: integrability and soliton interaction in non-Kerr media, Phys. Rev. E 60 (3) (1999) 3314.
[46] N. Raza, A. Javid, Dynamics of optical solitons with Radhakrishnan–Kundu–Lakshmanan model via two reliable integration schemes, Optik 178 (2019) 557–566.
[47] N. Ozdemir, H. Esen, A. Secer, M. Bayram, T.A. Sulaiman, A. Yusuf, H. Aydin, Optical solitons and other solutions to the Radhakrishnan–Kundu–Lakshmanan, Optik 242 (2021) 167363.
[48] A. Biswas, 1-soliton solution of the generalized Radhakrishnan–Kundu–Lakshmanan equation, Phys. Lett. A 373 (30) (2009) 2546–2548.
[49] H. Eldidamony, H.M. Ahmed, A. Zaghrout, Y. Ali, A.H. Arnous, Mathematical methods for construction new soliton solutions of Radhakrishnan–Kundu–Lakshmanan equation, Alex. Eng. J. 61 (9) (2022) 7111–7120.
[50] A.M. Elsherbeny, R. El–Barkouky, H.M. Ahmed, R.M. El-Hassani, A.H. Arnous, Optical solitons and another solutions for Radhakrishnan–Kundu–Lakshmanan equation by using improved modified extended tanh-function method, Opt. Quantum Electron. 53 (12) (2021) 1–15.
[51] B. Ghanbari, J. Gómez-Aguilar, Optical soliton solutions for the nonlinear Radhakrishnan–Kundu–Lakshmanan equation, Modern Phys. Lett. B 33 (32) (2019) 1950402.
[52] M. Ozisik, A. Secer, M. Bayram, A. Yusuf, T.A. Sulaiman, On the analytical optical soliton solutions of perturbed Radhakrishnan–Kundu–Lakshmanan model with Kerr law nonlinearity, Opt. Quantum Electron. 54 (6) (2022) 1–17.
[53] A. Biswas, Y. Yildirim, E. Yasar, M.F. Mahmood, A.S. Alshomrani, Q. Zhou, S.P. Moshokoa, M. Belic, Optical soliton perturbation for Radhakrishnan–Kundu–Lakshmanan equation with a couple of integration schemes, Optik 163 (2018) 126–136.
[54] A. Biswas, M. Ekici, A. Sonmezoglu, A.S. Alshomrani, Optical solitons with rRadhakrishnan–Kundu–Lakshmanan equation by extended trial function scheme, Optik 160 (2018) 415–427.
[55] A. Biswas, Optical soliton perturbation with Radhakrishnan–Kundu–Lakshmanan equation by traveling wave hypothesis, Optik 171 (2018) 217–220.
[56] Sirendaoreji, Unified Riccati equation expansion method and its application to two new classes of Benjamin-Bona-Mahony equations, Nonlinear Dynam. 89 (1) (2017) 333–344.
[57] E.M. Zayed, R.M. Shohib, M.M. El–Horbaty, A. Biswas, M. Asma, M. Ekici, A.K. Alzahrani, M.R. Belic, Solitons in magneto–optic waveguides with quadratic–cubic nonlinearity, Phys. Lett. A 384 (25) (2020) 126456.
[58] G. Akram, M. Sadaf, S. Arshed, F. Sameen, Bright, dark, kink, singular and periodic soliton solutions of Lakshmanan–Porsezian–Daniel model by generalized projective riccati equations method, Optik 241 (2021) 167051.
[59] C. Yong, L. Biao, New exact travelling wave solutions for generalized Zakharov–Kuznetsov equations using general projective Riccati equation method, Commun. Theor. Phys. 41 (1) (2004) 1.
[60] M. Ozisik, A. Secer, M. Bayram, H. Aydin, An encyclopedia of Kudryashov's integrability approaches applicable to optoelectronic devices, Optik 265 (2022) 169499.
[61] H. Esen, A. Secer, M. Ozisik, M. Bayram, Dark, bright and singular optical solutions of the Kaup–Newell model with two analytical integration schemes, Optik 261 (2022) 169110.
[62] M.Z. Elsayed, A.A. Khaled, The generalized projective riccati equations method and its applications for solving two nonlinear PDEs describing microtubules, Int. J. Phys. Sci. 10 (13) (2015) 391–402.
[63] S.D. Zhu, The generalizing riccati equation mapping method in non-linear evolution equation: application to (2+ 1)-dimensional Boiti–Leon–Pempinelle equation, Chaos Solitons Fractals 37 (5) (2008) 1335–1342.
[64] S. Guo, L. Mei, Y. Zhou, C. Li, The extended Riccati equation mapping method for variable-coefficient diffusion–reaction and mKdV equations, Appl. Math. Comput. 217 (13) (2011) 6264–6272.
[65] Z. Li, Z. Dai, Abundant new exact solutions for the $(3+1)$-dimensional Jimbo–Miwa equation, J. Math. Anal. Appl. 361 (2) (2010) 587–590.